WATER IN LUNAR PYROCLASTIC DEPOSITS: LINKING ORBITAL OBSERVATIONS TO INTERIOR PROCESSES.

S. Li[1] and R. E. Milliken[1], [1]Department of Earth, Environmental, and Planetary Sciences, Brown University, RI, 02912, shuai_li@brown.edu

Introduction: Water (OH and/or H_2O) on the lunar surface and preserved in lunar materials can record information about solar wind, cosmic ray, impact, and lunar interior processes. In particular, understanding if any lunar surface hydration signatures can be linked to endogenous (e.g., magmatic) sources has the potential to inform us of the nature and distribution of volatiles in the lunar interior.

Water content of Apollo samples have been studied via pyrolysis [1] and other more direct [2] approaches. Over one hundred measurements of major constituents of Apollo samples show that the water content in bulk samples is on the order of 44.3 ± 83.4 (2σ) ppm and has an upper limit 63.0 ± 96.7 (2σ) ppm (Figure 1). Though such measurements may suffer from terrestrial contamination, they still provide a useful constraint for comparison against estimates based on remote sensing data (e.g., M^3 reflectance spectra).

In addition, measurements of melt inclusions in Apollo 17 orange glass reach ~1400 ppm [3], whereas diffusion modeling of water in Apollo 15 green glass indicates pre-eruptive contents of 745 pprm [2]. Partial melting models for water in lunar apatite suggest sources with at least 64 ppb – 5 ppm water [4]. Questions also remain as to how much water is consistent with current petrologic and magma ocean models, which suggest low values [5].

Orbitally-acquired reflectance spectra provide an additional method of assessing lunar hydration, though it must first be determined what the sources are of any such signatures. Volcanic glasses in pyroclastic deposits represent materials sourced from deep within the lunar interior (~400 – 500 km) that formed as explosive fire fountains enriched in volatiles [6]. Thus orbital mapping of water in lunar pyroclastic deposits can provide large-scale information on the distribution of water in the lunar interior and at sites not sampled during the Apollo missions.

Here we examine lunar surface hydration mapped with new thermally-corrected M^3 data (~280 m/pixel) [11] to assess which, if any, signatures may be related to water from the lunar interior. Lunar surface hydration mapped at latitudes between ±30° is expected to be low and within the range measured for Apollo bulk soil samples. In contrast, water in lunar pyroclastic deposits may deviate from this trend depending on volatile content of magma source regions, concentration mechanisms, degassing history, and post-emplacement modification.

Methods: In our previous work we demonstrated that Hapke's Effective Single Particle Absorption Thickness (ESPAT), calculated at ~2.9 μm from single scattering albedo spectra, can be used as a linear proxy for water content [11]. Laboratory experiments and numerical simulations were used to determine specific H_2O% - ESPAT trends in order to estimate water content directly from ESPAT values. Reflectance spectra were measured for a series of synthetic hydrated basaltic glasses and terrestrial anorthosite samples of different particle sizes and water contents to determine relevant H_2O%-ESPAT trends and to examine how such trends are affected by composition and/or particle size.

The H_2O%-ESPAT trend can also be numerically simulated if the absorption coefficient for a material (e.g., hydrated glass) is known. A relationship between water concentration (c) and the absorbance (A) at ~2.8 μm was derived for silicate glasses by Stolper [12]:

$$c = (18.02 \cdot A) / (d \cdot \rho \cdot \varepsilon) \quad (1)$$

where d, ρ, and ε are the thickness, density, and extinction coefficient of silicate glasses, respectively; in this work we adopted the average value of ε = 67 L/mol·cm reported by [12] for a variety of glass compositions. Using radiative transfer theory [13], we can determine the relationship between A and ESPAT to convert the above equation to a function relating H_2O% and ESPAT. An H_2O% - ESPAT trend can then be simulated for different particle sizes once the value of ε is known or assumed.

Results and Discussion: Experimental results show that H_2O% = 1.8·ESPAT for basaltic glasses and terrestrial anorthosits with particle sizes <45 μm, regardless of composition (Figure 2). Our simulations for particle sizes <45 μm based on Eq. (1) show an identical H_2O% - ESPAT trend (Figure 2), though additional experiments are required to verify the simulated trends at other particle sizes.

Water contents for bulk lunar regolith between ±30° latitude were derived from our mapped ESPAT values to compare against measurements from Apollo samples (Figure 1). The mean particle size (~60-80 μm) measured from Apollo samples [14] was used to estimate the proper H_2O% - ESPAT slope; assuming that smaller particles dominate the M^3 spectra would yield higher estimated water contents. As shown in Fig. 1, estimated water contents of lunar soil using M^3 data

are in good agreement with lab measurements of water content in Apollo samples, suggesting an upper limit of ~100 ppm in typical lunar soil at non-polar latitudes.

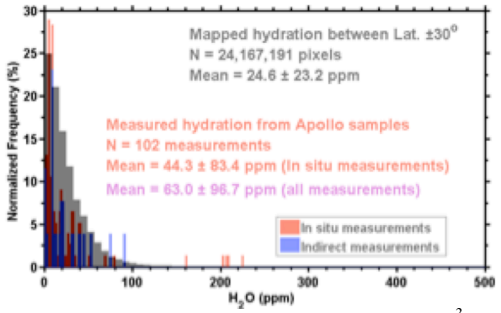

Figure 1. Lunar surface water estimates from M^3 data compared to measurements from Apollo samples showing broad agreement for typical lunar soils. ~100 ppm is considered an upper limit.

The ESPAT value associated with this upper limit, here considered the 'background' spectral signature of lunar surface hydration, was subtracted from the ESPAT values for eleven large pyroclastic deposits [15] at similar latitudes. These pyroclastic deposits exhibit an 'excess' ESPAT value compared to surrounding lunar soils, even if we assume the unlikely case that the optically dominant average particle size for these deposits is 100 times larger than that of typical lunar soils (Fig. 2). We interpret this 'excess' hydration signature to reflect water in volcanic glass that is sourced from the lunar interior.

The large pyroclastic deposits exhibit a wide range of excess ESPAT values (Fig. 2). This may be in part due to differences in average particle size for these deposits, but volcanic glasses from Apollo 11, 15, and 17 samples exhibit similar mean particle size ranges (30 – 40 μm). We estimated the H_2O% - ESPAT trend for two extreme particle size scenarios (15 μm and 150 μm) in order to bracket the absolute water abundances implied by the absorption features observed in M^3 data. These scenarios translate into min and max water contents of ~34 and ~2000 ppm, respectively, for the bulk deposits. For a more realistic case (particle size 30 – 40 μm) the pyroclastics may contain 150 ppm – 900 ppm water depending on the deposit in question. If the pyroclastic deposits have similar particle size distributions (and thus similar H_2O% - ESPAT trends), the different ESPAT values would indicate different water contents for each deposit.

Conclusions:

We have assessed lunar surface hydration using orbital observations and supporting laboratory experiments and simulations. Water content values mapped between ±30° latitude using M^3 data are typically low and consistent with water contents measured from Apollo bulk soil samples. However, 'excess' hydration is observed in eleven large pyroclastic deposits within this same latitude range, and we interpret at least part of this hydration to be associated with volcanic glass and thus indicative of water from the lunar interior.

Quantitative estimates of this component of endogenous lunar water are uncertain due to limited knowledge on the particle size distribution of these pyroclastics at the optical surface. If we assume particle size distributions similar to those measured from Apollo 11, 15, and 17 volcanic glasses then our observations imply that large pyroclastic deposits may exhibit striking differences in water content. If confirmed, such variation could indicate heterogeneous volatile distribution in the lunar interior, different degassing histories, and/or variable modification by post-emplacement processes.

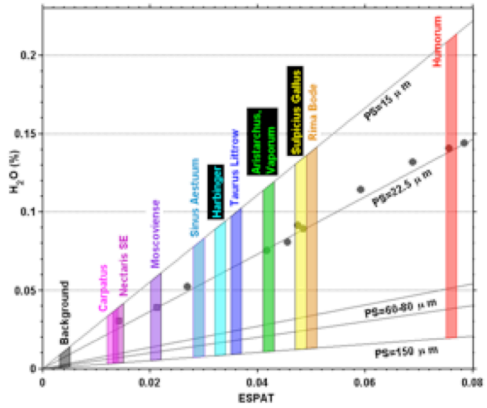

Figure 2. Gray lines: simulated H_2O% - ESPAT trends for different particle sizes (PS); experimental data for basaltic glasses (squares) and anorthosite (circles) are shown. Color bars are 'background' removed mean ESPAT values for 11 large pyroclastic deposits with H_2O ranges based on 2 particle size scenarios. Note that H_2O for pyroclastic is above 0 even for the largest particle size scenario.

References: [1]. Friedman, I. *et al.* (1971) *LPSC Proc.* 1407. [2]. Saal, A. E. *et al.* (2008). *Nature* **454**. [3]. Hauri, E. H. *et al.* (2011). *Science* **333**. [4]. McCubbin, F. M. *et al.* (2010). *PNAS* **107**. [5]. Elkins-Tanton, L. T. & Grove, T. L. (2011). *EPSL* **307**. [6]. Heiken, G. H. *et al.* (1974). *GCA* **38**. [7]. Pieters, C. M. *et al.* (2009). *Science* **326**. [8]. Feldman, W. C. *et al.* (1998). *Science* **281**. [9]. Clark, R. N. (2009). *Science* **326**. [10]. Sunshine, J. M. *et al.* (2009). *Science* **326**. [11]. Li, S. & Milliken, R. E. (2013) *LPSC*. 1337. [12]. Stolper, E. (1982). *CMP* **81**. [13]. Hapke, B. (1981). *JGR* **86**. [14]. Heiken, G. H. *et al.* (1991). Cambridge University Press. [15]. Gaddis, L. R. *et al.* (2003). *Icarus* **161**.